

Predicting Muon Fluxes and Seasonal Variations in Underground and Underwater Labs Using MUTE

William Woodley

Supervisor: Prof. Marie-Cécile Piro
21 June 2023



**UNIVERSITY
OF ALBERTA**



Arthur B. McDonald
Canadian Astroparticle Physics Research Institute

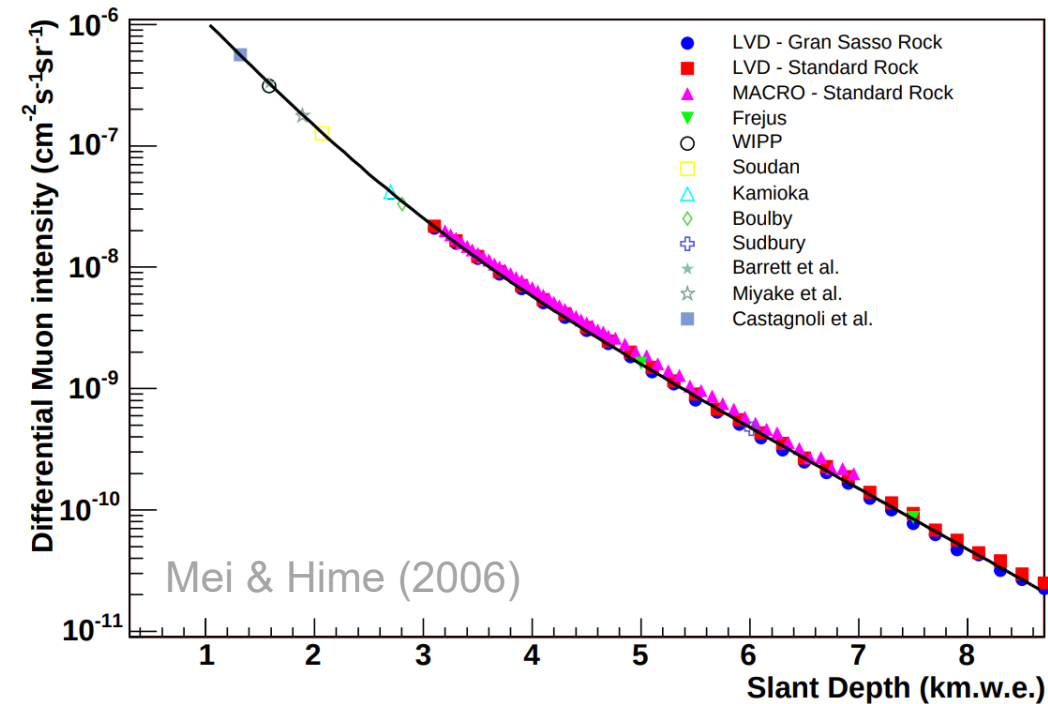
Depth-Intensity Relations

- Depth Intensity Relations [2, 3] are a common way of calculating underground muon fluxes.
- Disadvantages:
 1. They are simple parametric fits.
 2. They are susceptible to statistical errors at deep slant depths.
 3. They are approximate and introduce systematic errors for $\theta > \sim 20^\circ$ [4].
- MUTE (**MU**on in**T**ensity cod**E**) solves all three of these problems.
- It is a computational tool written in Python that calculates muon spectra underground.

Continuous
Losses

Discrete
Losses

$$I(h) = I_1 e^{-h/\lambda_1} + I_2 e^{-h/\lambda_2}$$

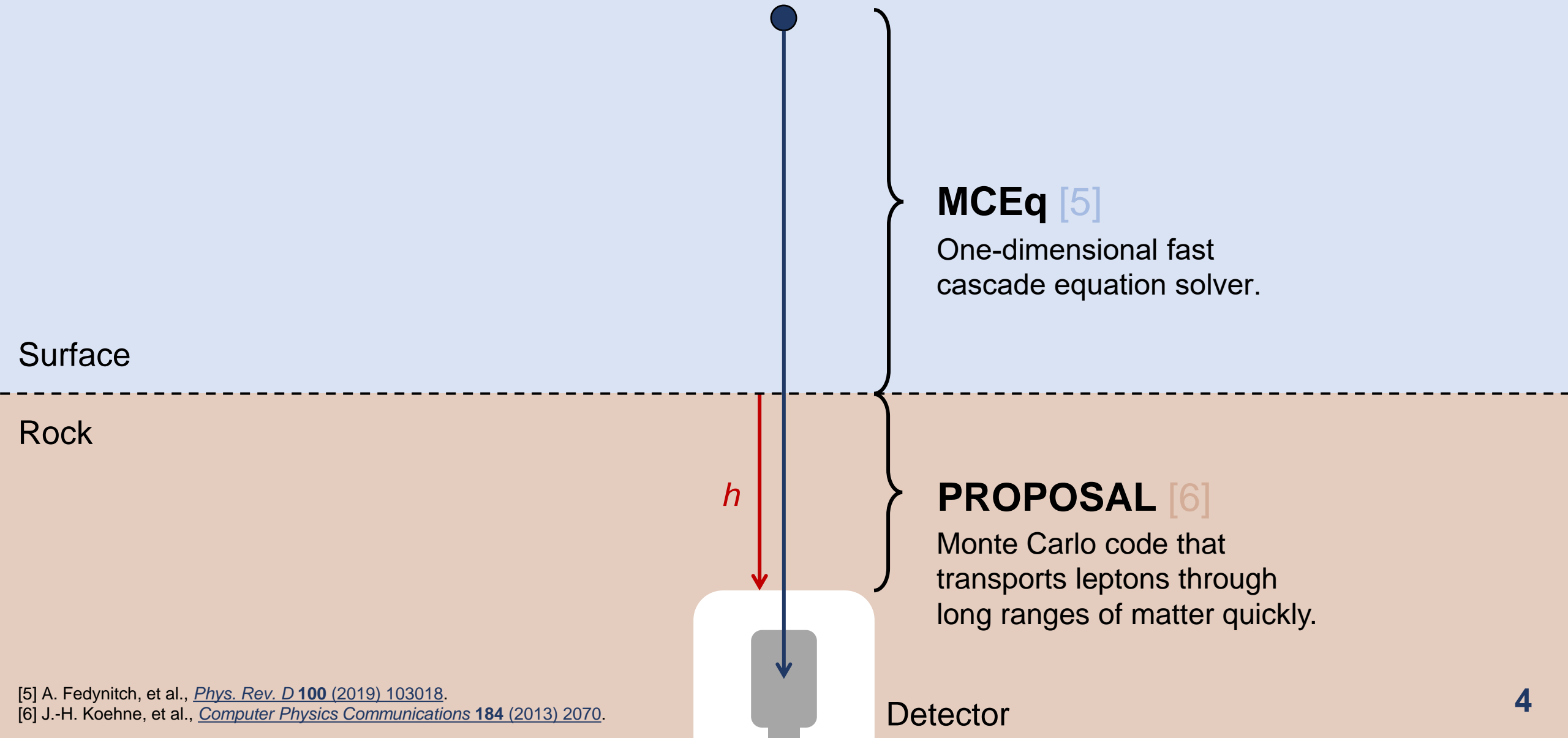


[2] D. Mei and A. Hime, *Phys. Rev. D* **73** (2006) 053004 [[astro-ph/0512125](#)].

[3] M. Crouch, in *ICRC*, vol. 6, p. 165, Jan., 1987.

[4] A. Fedynitch, W. Woodley and M.-C. Piro, *ApJ* **928** (2022) 27.

Method – Overview



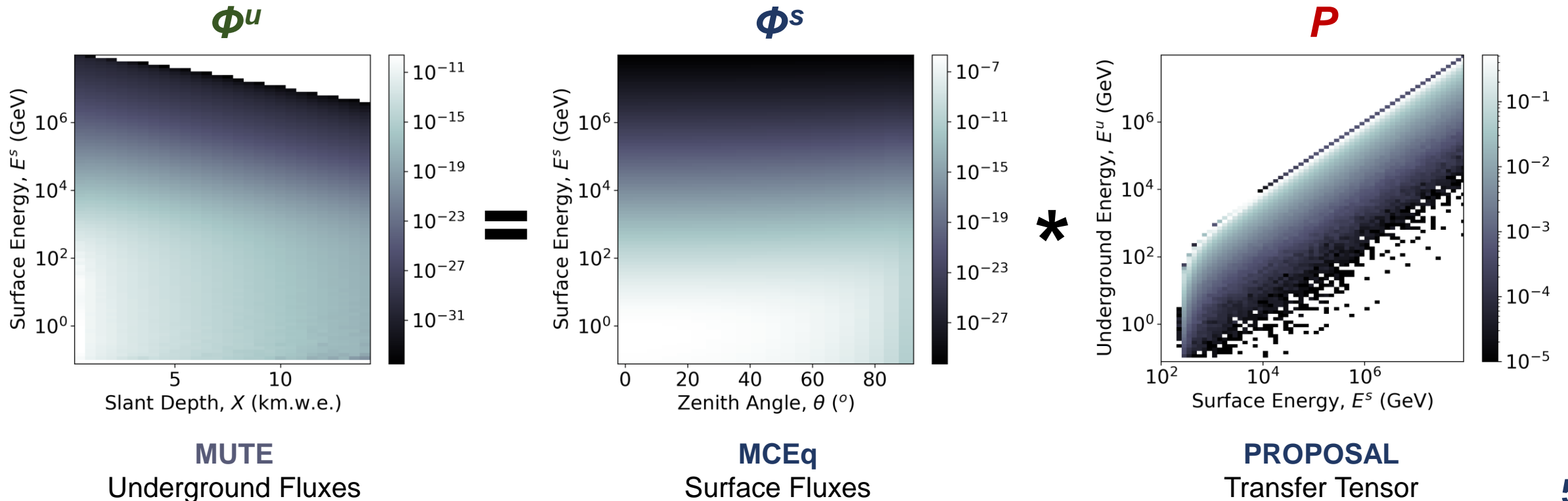
[5] A. Fedynitch, et al., *Phys. Rev. D* **100** (2019) 103018.

[6] J.-H. Koehne, et al., *Computer Physics Communications* **184** (2013) 2070.

Method – Convolution

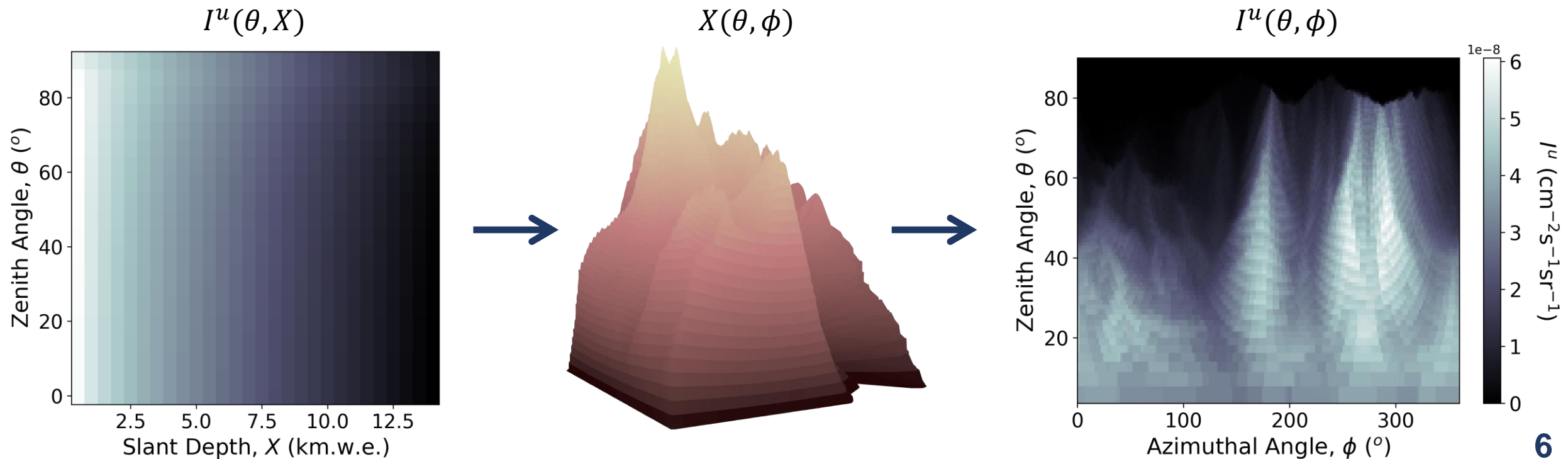
- A convolution is performed to calculate underground fluxes:

$$\Phi^u(E_j^u, X_k, \theta_k) = \sum_i \Phi^s(E_i^s, \theta_k) P(E_i^s, E_j^u, X_k) \left(\frac{\Delta E_i^s}{\Delta E_j^u} \right)$$



Method – Labs under Mountains

- Underground intensities for mountains are first calculated on a grid of constant zenith angles and slant depths.
- Using a map of the mountain profile, these intensities are then interpolated to the slant depths $X(\theta, \phi)$ that define the mountain.



Method – Surface Flux Models

- The user can switch out models to be used in MCEq for surface flux calculations.

DDM [7]:

- Data-driven model for hadronic interactions.
- Uses low-energy accelerator data.
- Extrapolates to higher energies using Feynman scaling.

[7] A. Fedynitch and M. Huber, *Phys. Rev. D* **106** (2022) 083018 [[2205.14766](#)].

[8] J.P. Yañez and A. Fedynitch, [2303.00022](#).

Method – Surface Flux Models

- The user can switch out models to be used in MCEq for surface flux calculations.

DDM [7]:

- Data-driven model for hadronic interactions.
- Uses low-energy accelerator data.
- Extrapolates to higher energies using Feynman scaling.

DAEMONFLUX [8]:

- Combines DDM and Global Spline Fit (GSF).
- Calibrated to muon flux and ratio data.
- Φ_ν uncertainties <10% up to 1 TeV.

[7] A. Fedynitch and M. Huber, *Phys. Rev. D* **106** (2022) 083018 [[2205.14766](#)].

[8] J.P. Yañez and A. Fedynitch, [2303.00022](#).

Method – Surface Flux Models

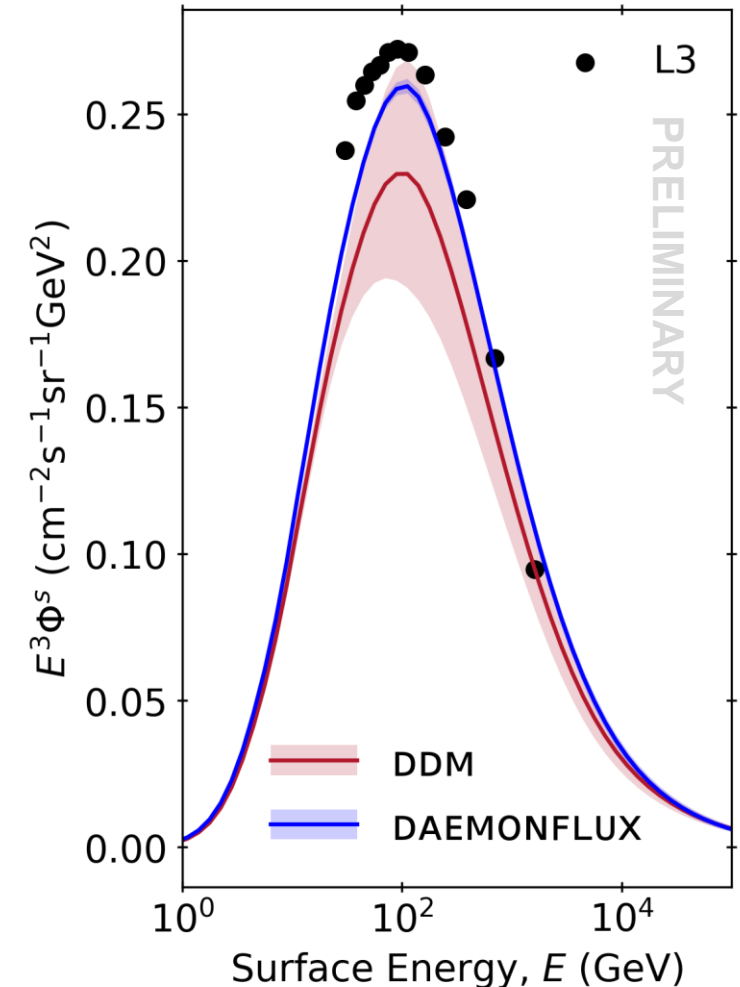
- The user can switch out models to be used in MCEq for surface flux calculations.

DDM [7]:

- Data-driven model for hadronic interactions.
- Uses low-energy accelerator data.
- Extrapolates to higher energies using Feynman scaling.

DAEMONFLUX [8]:

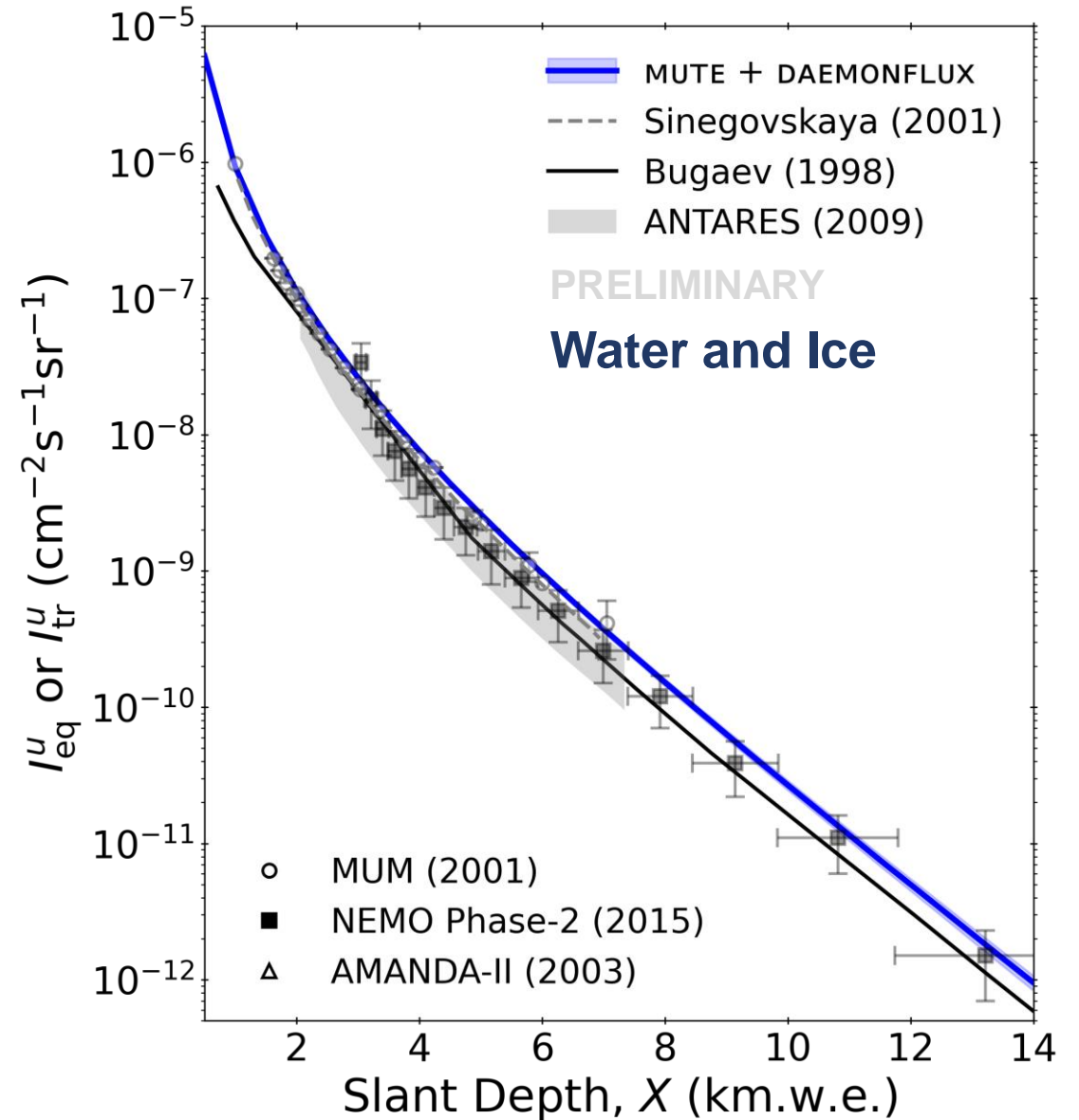
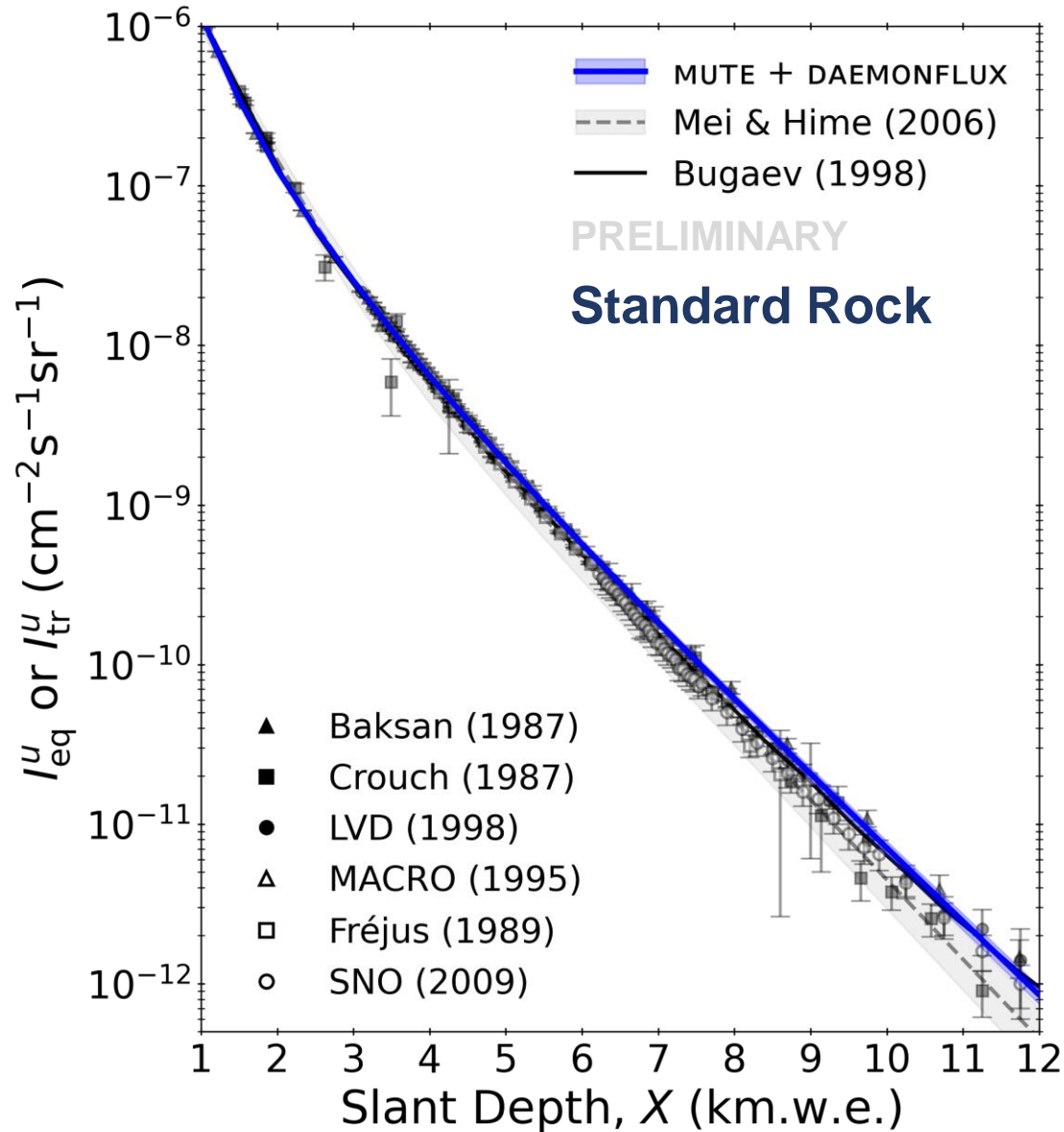
- Combines DDM and Global Spline Fit (GSF).
- Calibrated to muon flux and ratio data.
- Φ_ν uncertainties <10% up to 1 TeV.



[7] A. Fedynitch and M. Huber, *Phys. Rev. D* **106** (2022) 083018 [2205.14766].

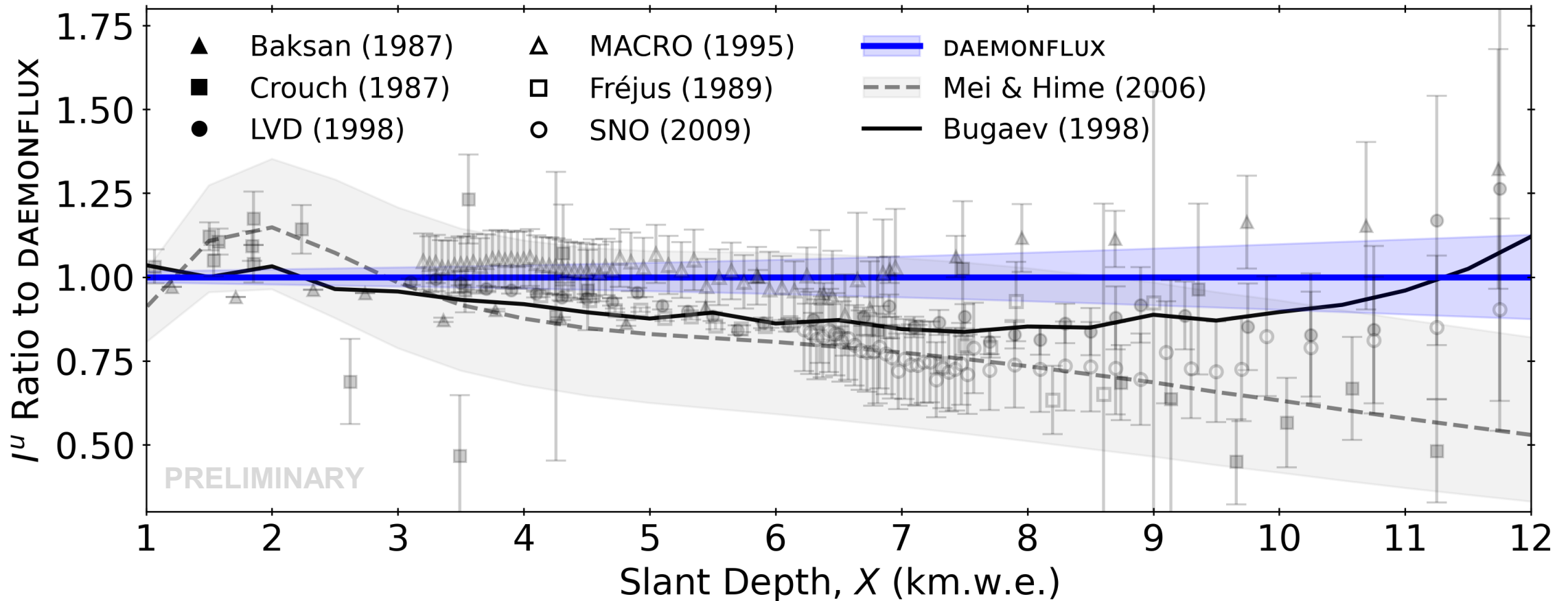
[8] J.P. Yañez and A. Fedynitch, [2303.00022](#).

Results – Vertical Underground Intensity



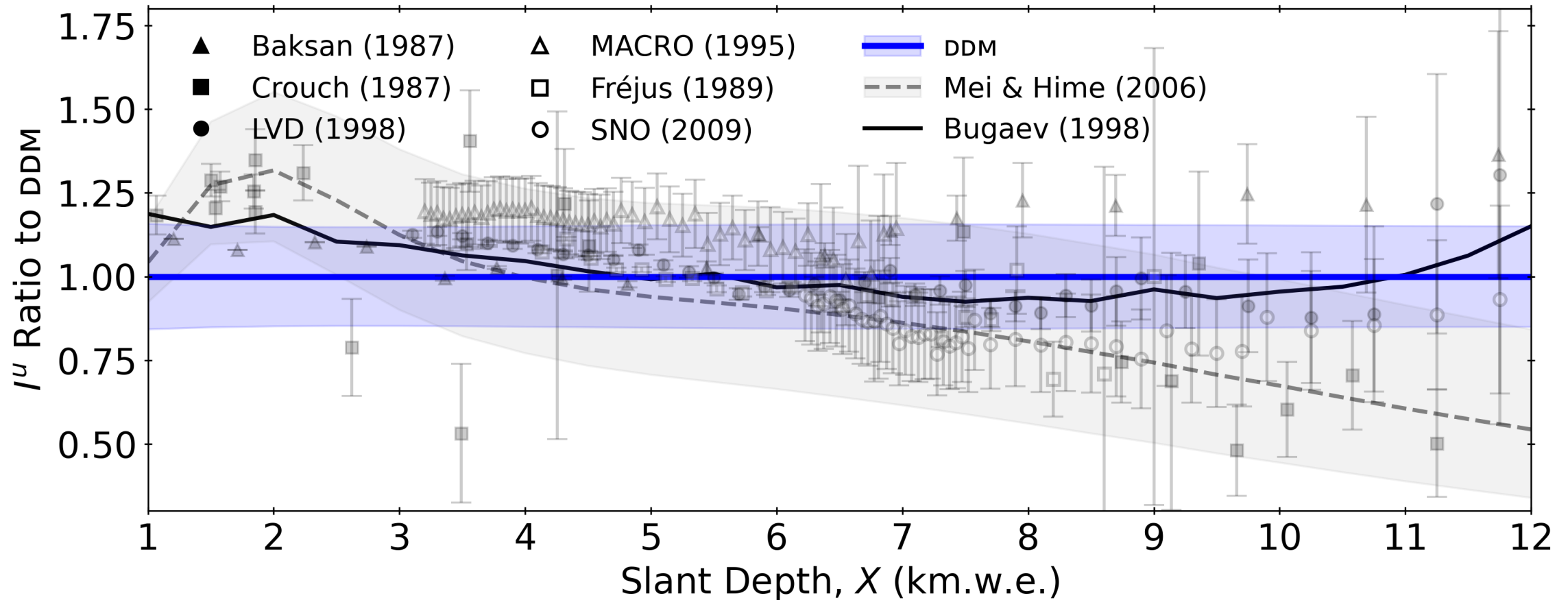
Results – Comparison to Data

- Uncertainties have been reduced from 15% to ~1% by using DAEMONFLUX.



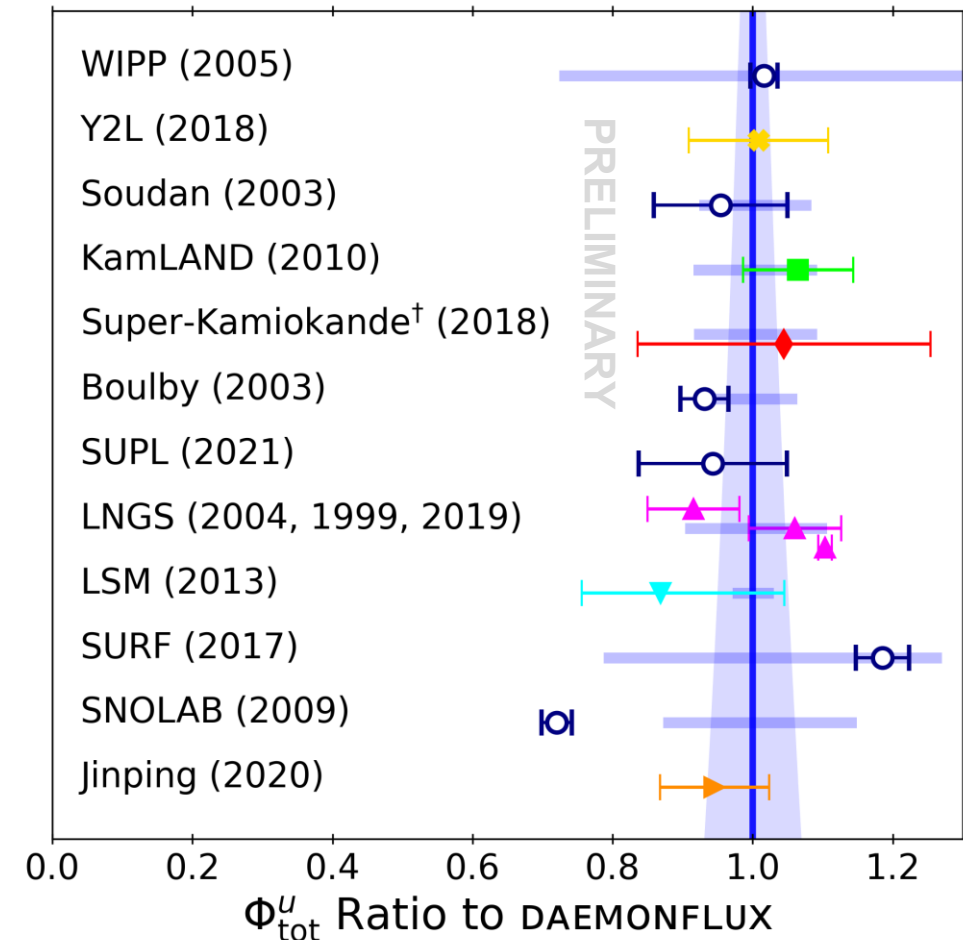
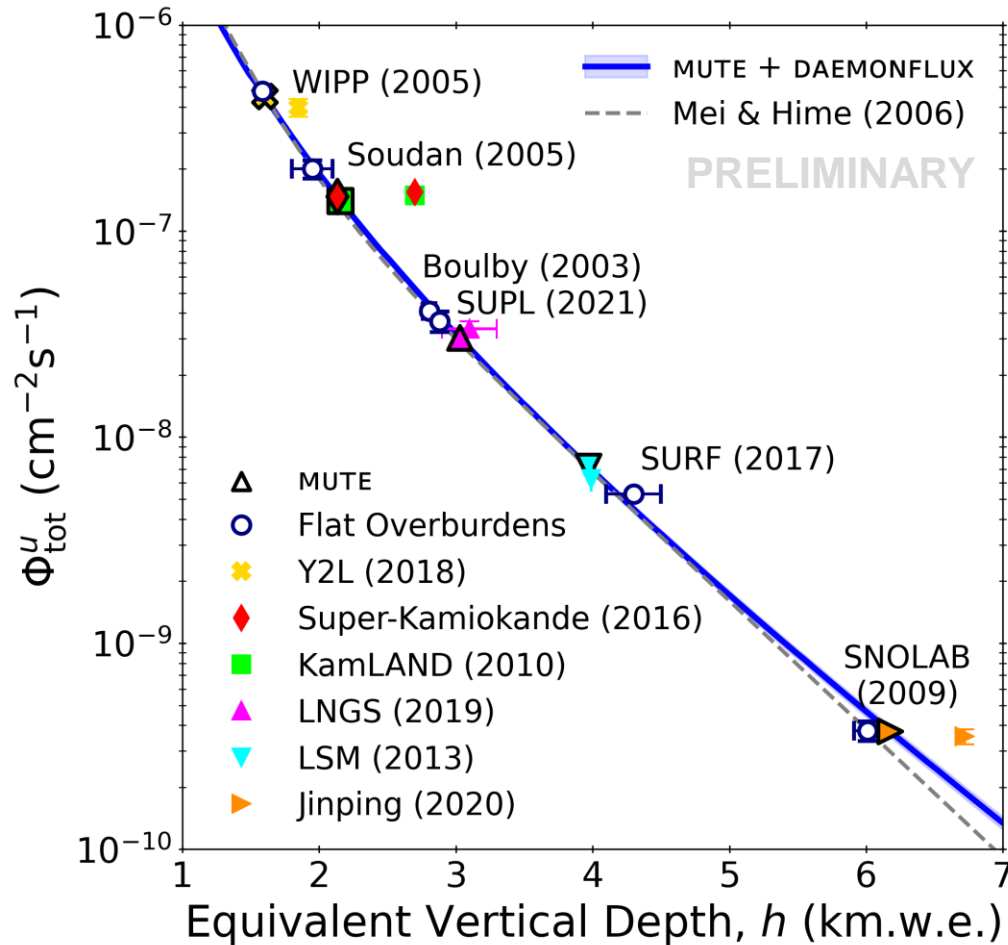
Results – Comparison to Data

- Uncertainties have been reduced from 15% to ~1% by using DAEMONFLUX.



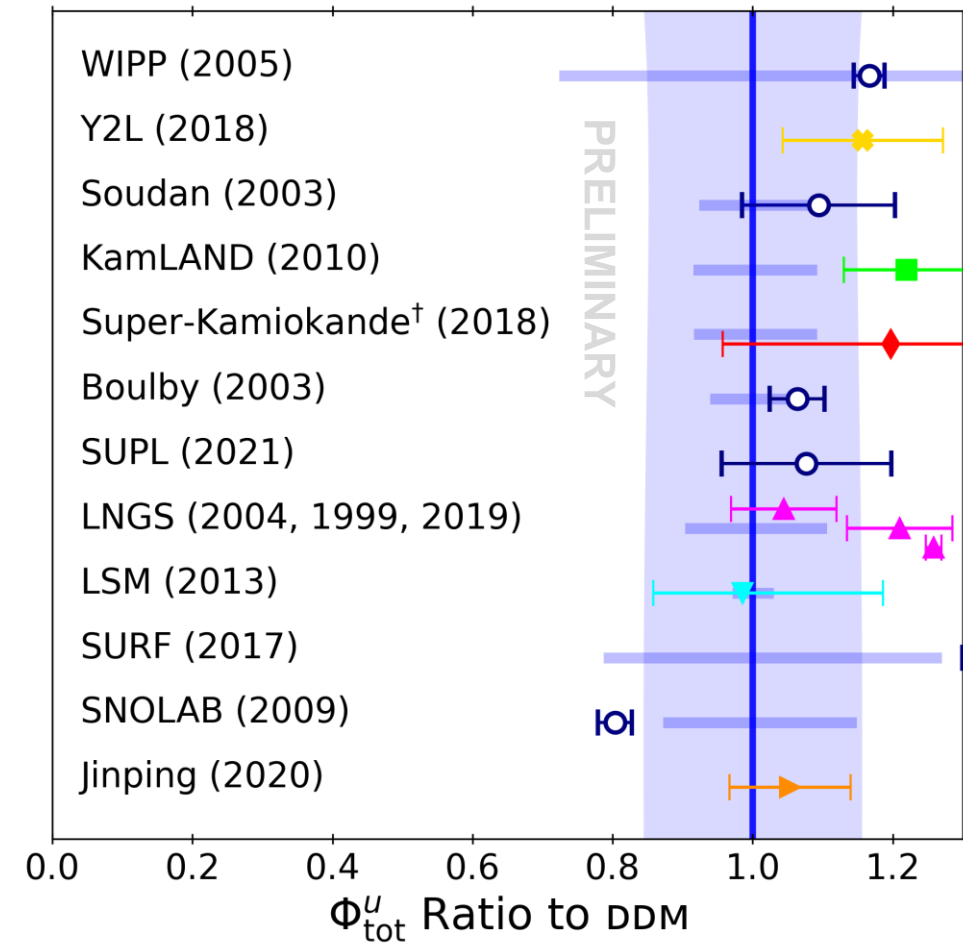
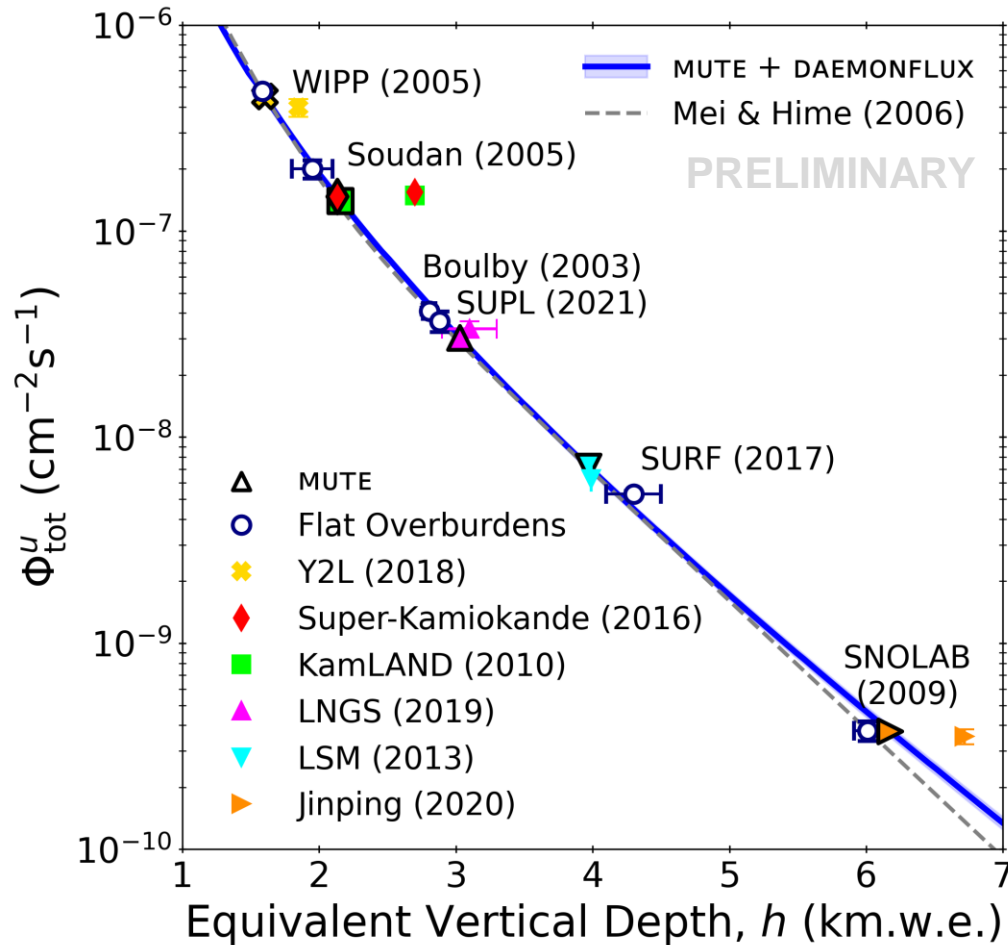
Results – Total Underground Flux

- Total flux calculations are consistent with measurements for labs under flat overburdens and mountains within theoretical errors in nearly every case.

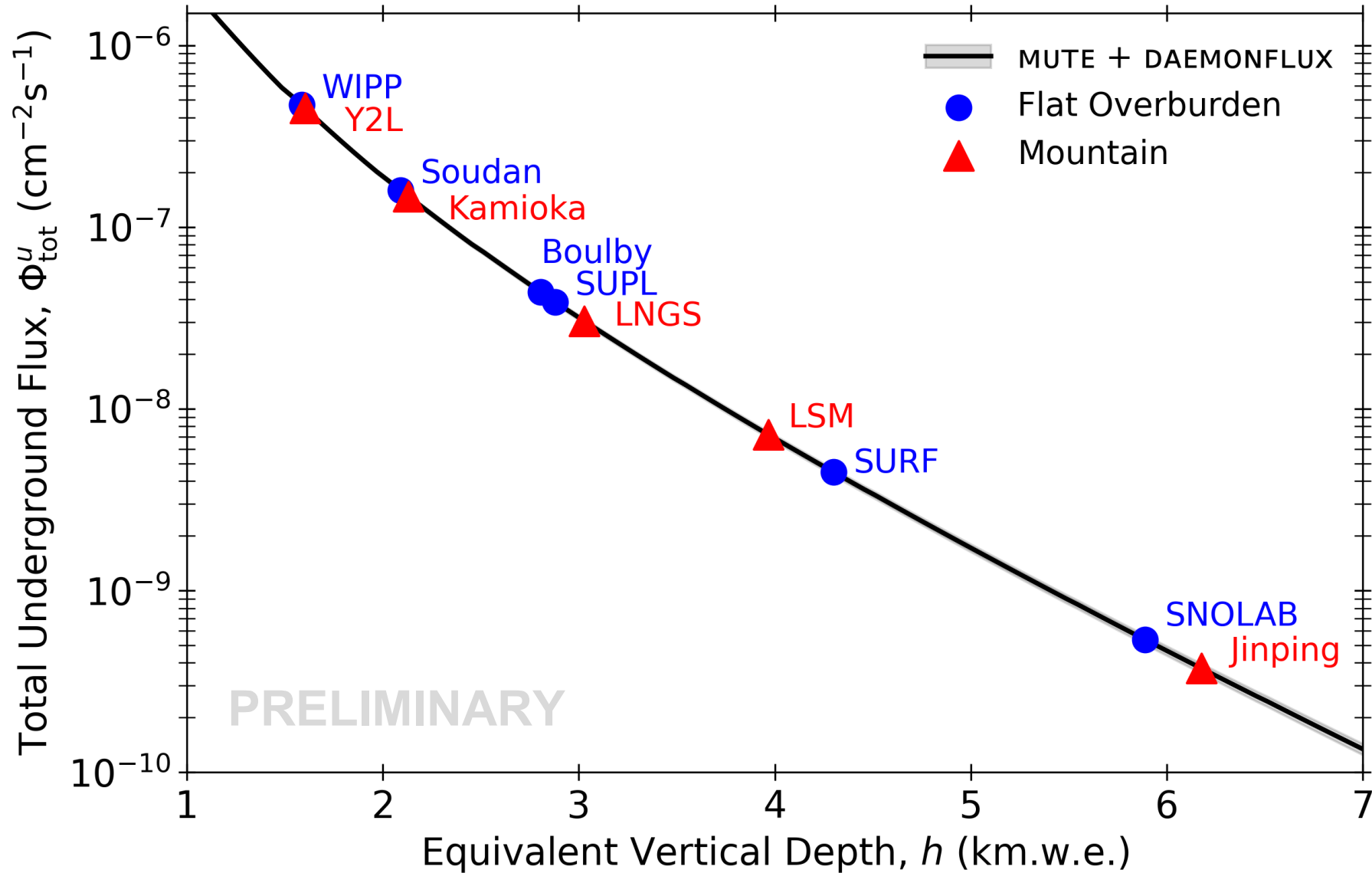


Results – Total Underground Flux

- Total flux calculations are consistent with measurements for labs under flat overburdens and mountains within theoretical errors in nearly every case.

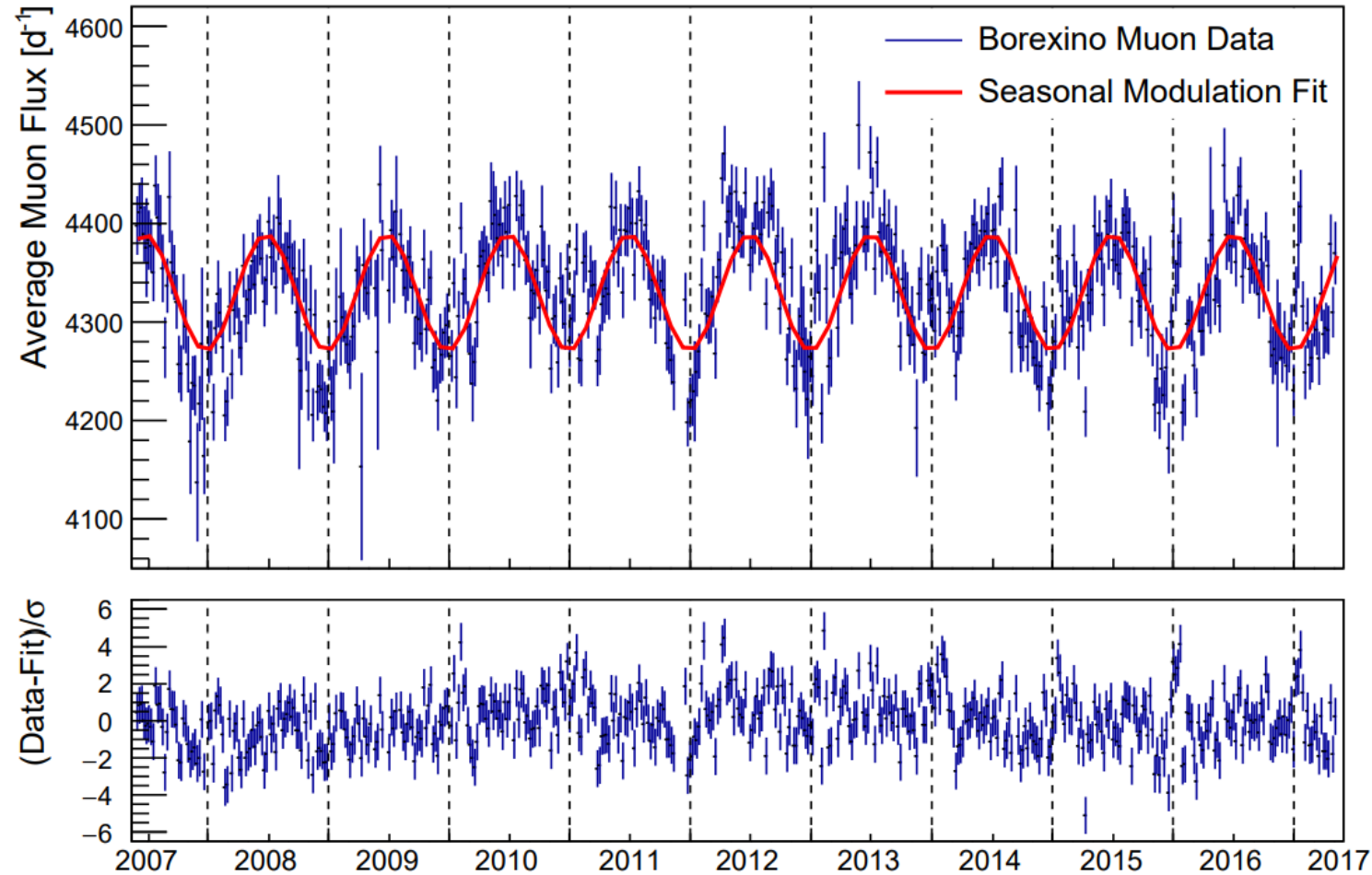


Results – Total Underground Flux



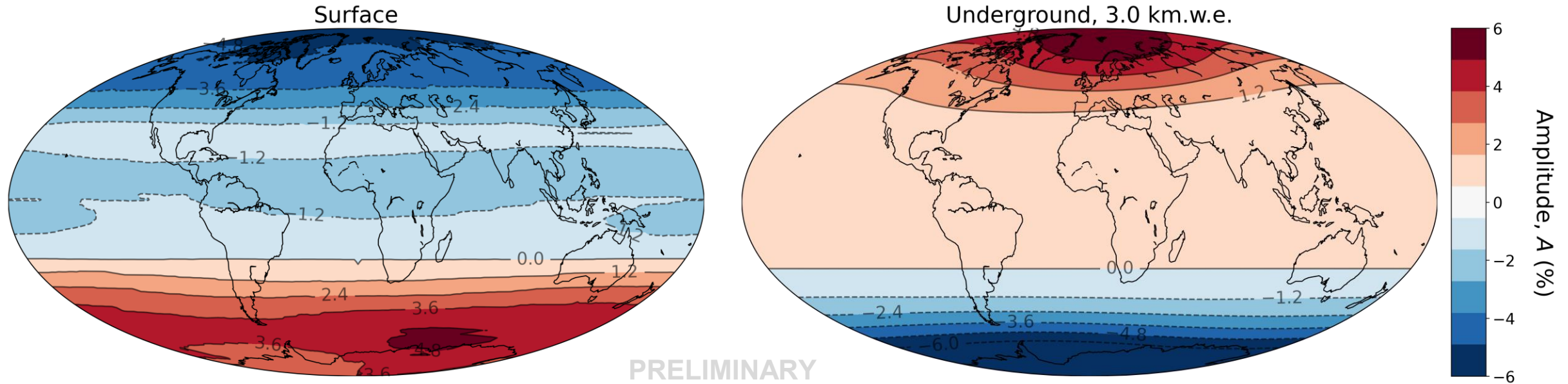
Seasonal Variations

- The phenomenon of seasonal modulations in the muon flux is well-known [9]:



Seasonal Variations – Results

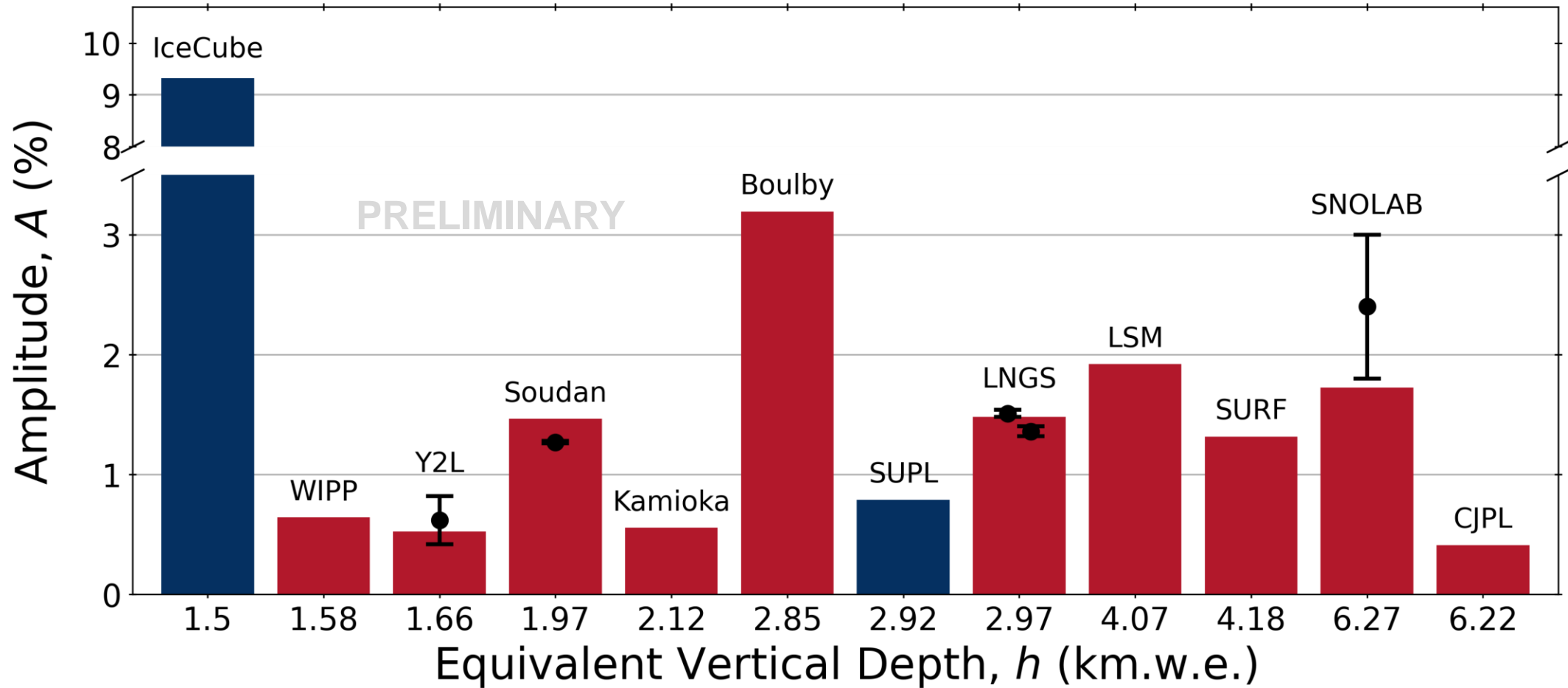
- I have calculated the amplitude of seasonal variations around the globe:



- The muon flux is **lower** at the surface in summer in the **northern hemisphere**.
- However, there are more higher-energy muons in the summer, which reach deeper underground. Therefore, the muon flux is **higher** underground in summer.

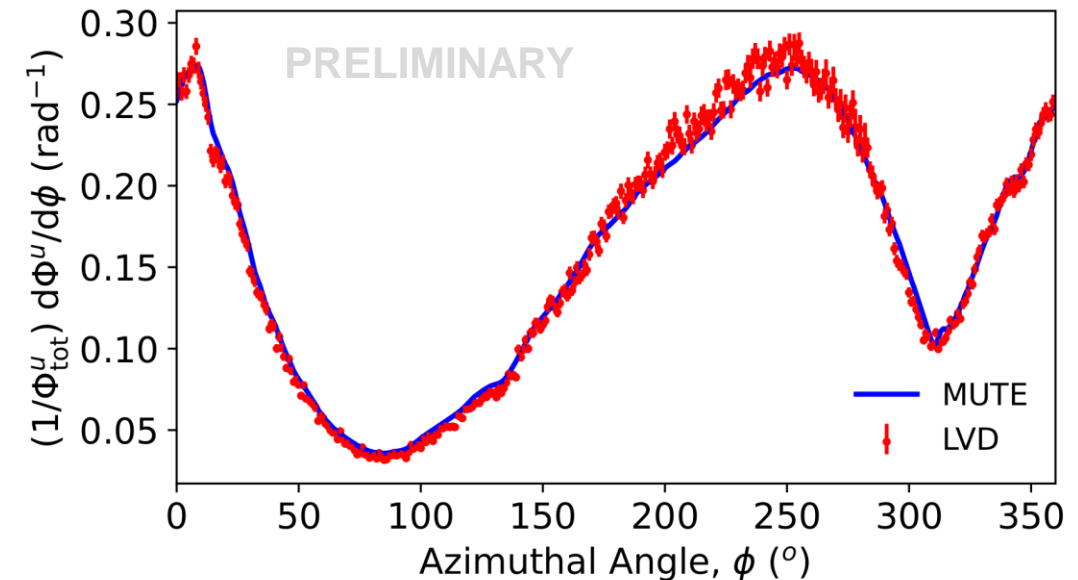
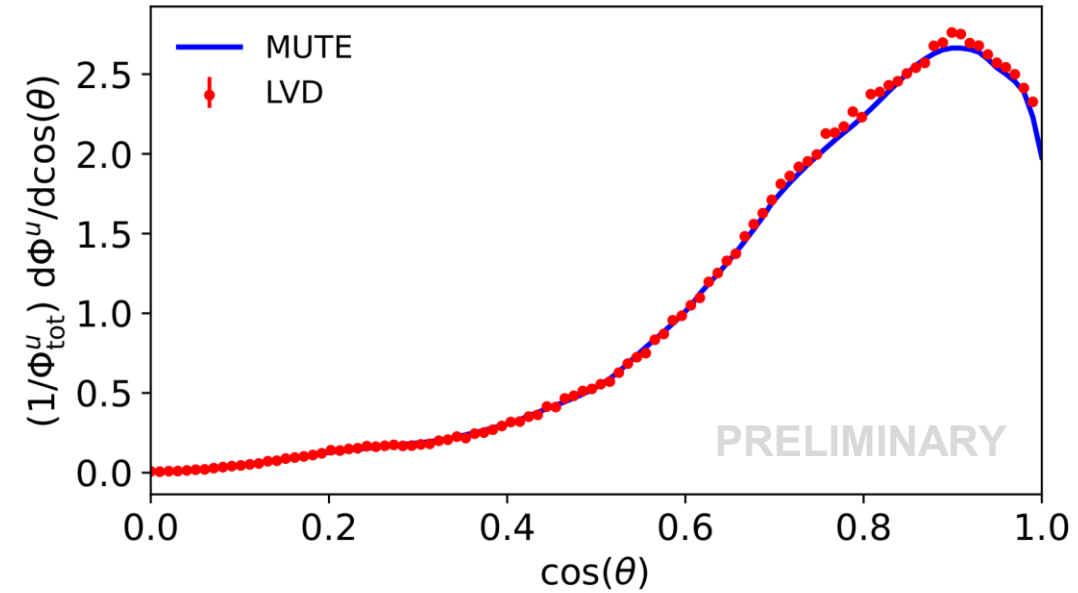
Seasonal Variations – Results

- MUTE can calculate seasonal variation amplitudes to high accuracy.



Applications – Angular Distributions

- MUTE can also calculate one-dimensional angular distributions for labs under mountains in the θ and ϕ directions.
- Results for the Gran Sasso mountain have been compared to data from the LVD experiment.
- We obtain very good agreement for the muon spectrum and flux, and for the shape of the mountain.
- This serves as a way of verifying the data analysis of the LVD experiment.



Conclusion

- MUTE is flexible, fast, and precise. It gives a full description of muon distributions underground and underwater, and can provide forward predictions for total muon fluxes.
- The results match experimental data very well for all physical observables. This can be used to cross-check data analyses.
- Uncertainties have been significantly reduced with the latest model, DAEMONFLUX.
- MUTE is public and available (`pip install mute`) to be used by experiments in labs under flat overburdens and mountains.

[doi:10.3847/1538-4357/ac5027](https://doi.org/10.3847/1538-4357/ac5027)

<https://github.com/wjwoodley/mute>

Thank you

Data References

8. PDG: Particle Data Group, [PTEP 2020 \(2020\) 083C01](#).
9. ANTARES (2009): ANTARES, [0911.3055](#).
10. AMANDA-II (2003): X. Bai *et al.*, in 28th International Cosmic Ray Conference, pp. 1373–1376, 5, 2003.
11. NEMO Phase-2 (2015): NEMO, [Astropart. Phys. 66 \(2015\) 1 \[1412.0849\]](#).
12. Sinigovskaya (2001): T.S. Sinigovskaya and S.I. Sinigovsky, [Phys. Rev. D 63 \(2001\) 096004 \[hep-ph/0007234\]](#).
13. MUM (2001): I.A. Sokalski, E.V. Bugaev and S.I. Klimushin, [Phys. Rev. D 64 \(2001\) 074015](#).
14. Y2L (2018): COSINE-100, [PoS ICRC2017 \(2018\) 883](#).
15. Super-K (2016): Hyper-Kamiokande, [1805.04163](#).
16. KamLAND (2010): KamLAND, [Phys. Rev. C 81 \(2010\) 025807 \[0907.0066\]](#).
17. Gran Sasso (2019): LVD, [Phys. Rev. D 100 \(2019\) 062002 \[1909.04579\]](#).
18. Fréjus (2013): EDELWEISS, [Astropart. Phys. 44 \(2013\) 28 \[1302.7112\]](#).
19. Jinping (2020): JNE, [Chin. Phys. C 45 \(2021\) 025001 \[2007.15925\]](#)
20. Tilav (2019): IceCube, [PoS ICRC2019 \(2020\) 894 \[1909.01406\]](#).
21. COSINE-100: COSINE-100, [2208.05158](#).
22. MINOS: MINOS Collaboration. [Phys. Rev. D 91 \(2015\) 112006](#).
23. Borexino: M. Agostini, *et al.*, [Journal of Cosmology and Astroparticle Physics 2019 \(2019\) 046](#).
24. SNO: C. Kyba, Ph.D. thesis, University of Pennsylvania, 2006.